Carbon nanotube reinforced PVAm/PVA blend FSC nanocomposite membrane for CO_2/CH_4 separation

Liyuan Deng, May-Britt Hägg*

Department of Chemical Engineering, Norwegian University of Science and Technology (NTNU), NO-7491 Trondheim, Norway

ARTICLE INFO

ABSTRACT

A carbon nanotube (CNT) reinforced polyvinyl amine/polyvinyl alcohol (PVAm/PVA) blend nanocomposite membrane with facilitated transport fixed-site-carriers (FSC) for CO_2/CH_4 separation was developed with the focus on improving membrane separation performance at elevated pressures and the challenges related to the up-scaling of the membrane for potential industrial applications. This nanocomposite membrane was prepared by dip-coating with the modified CNTs dispersed uniformly in a hydrophilic PVAm/PVA blended solution with a precise control of the coating layer thickness (coating layer thickness 0.5–2.5 μm). Membranes with an up-scaled size (300 × 300 mm) were prepared. A selectivity of CO_2/CH_4 up to 45 and a CO_2 permeance of up to 0.35 m^3 (STP)/m^2 h bar were documented in the low pressure range (2–5 bar). With the addition of a small amount of CNTs (1.0 wt.%), the membrane showed an enhanced water swelling, capacity as well as good durability against the compaction effect in operations at elevated pressures. The CO_2 permeance of the CNTs reinforced nanocomposite membranes improved significantly compared to its counterpart membrane without CNTs, while the CO_2/CH_4 selectivity remained similar. The effects of increased pressure (up to 15 bar) on membrane separation performance were investigated in the same way. The SEM images of the nanocomposite membrane confirmed that the CNTs and PVAm/PVA blend polymer were compatible.

© 2014 Elsevier Ltd. All rights reserved.

1. Introduction

Although there has been growing concern about global warming over the last decade, the concentration of carbon dioxide in the atmosphere surpassed the milestone level of 400 parts per million (ppm) for the first time in human history in May 2013. More effective technologies are required for capturing CO_2 from various sources. Being energy-saving, environment-friendly, low-cost and with a small footprint, membrane separation has great potential for becoming a green and efficient CO_2 capture technology. However, the separation performance of current commercial membranes is relatively low, and is judged to be not yet sufficient for the membrane separation process to compete with the most commonly used amine absorption processes, especially in medium to large-scale applications. For separations at high pressures, such as the natural gas sweetening process, penetrant-induced plasticization, physical aging and conditioning are some additional challenges (Adewole et al., 2013; Zhang et al., 2013). In our previous work, polyvinyl amine/polyvinyl alcohol (PVAm/PVA) blend fixed-site-carrier (FSC) membranes were investigated and reported to have an excellent CO_2 separation performance, which is compatible to amine absorption for a CO_2/CH_4 gas mixture (Deng and Hägg, 2010b; Deng et al., 2006). The membranes have good mechanical strength and stability (Deng and Hägg, 2008, 2010a). No pore filling of the support material (polysulfone) was found after a test of up to 25 bar. PVAm and PVA are very compatible polymers. The PVAm/PVA blend polymer was proven to be homogeneous (Deng et al., 2009). For example, the DSC graph of the PVAm/PVA blend shows only one melting point (Tm) that is different from those of PVAm and PVA. By the entanglement of PVAm with PVA chains in the blend membrane, amino groups in PVAm work as CO_2 facilitated transport carriers, while PVA offers an enhanced polymeric network with good membrane forming properties. The reversible CO_2 hydration reactions initiated by the weak basic amino carriers in the membrane selective layer facilitate the CO_2 transport, resulting in both high permeability and selectivity of CO_2 over other gases. Considering that amino groups are not consumed during the reversible reactions, they are playing the role of catalysts for the CO_2 hydration reactions, and the final reactions can therefore be illustrated with Eq. (1):

$$H_2O + CO_2 \overset{+NH_2}{\rightleftharpoons} H^+ + HCO_3^- \tag{1}$$

* Corresponding author.
E-mail addresses: deng@nt.ntnu.no (L. Deng), hagg@nt.ntnu.no, may-britt.hagg@chemeng.ntnu.no (M.-B. Hägg).

Accordingly, the transport of CO_2 through the PVAm/PVA blend membrane is believed to be in the form of bicarbonate ions, hence exhibiting a high CO_2 permeance due to the fact that the diffusion of ions in liquid or swollen hydrogel can be several orders of magnitude greater than those of gases in a solid (Cussler, 1997; Kim et al., 2013; Sandru et al., 2010; Deng and Hägg, 2010a; Liu et al., 2008). The common challenges for membranes at high pressure operations are therefore not relevant in this type of FSC membranes. The drawbacks are, however, that the separation performance of the membranes depends strongly on the membrane swelling conditions, while the swelling in the membrane causes an unavoidable loss of mechanical strength. In addition, the compaction effect at elevated or high pressures diminishes the membrane swelling capacity, and therefore reduces the diffusion rate. The aim of this current work has thus been to tailor the PVAm/PVA blend membrane to deal with these drawbacks so as to further improve the FSC membrane permeation performance, as well as the mechanical properties for CO_2/CH_4 separation at elevated pressures. A carbon nanotube (CNT) reinforced PVAm/PVA (CNT-PVAm/PVA) nanocomposite membrane was designed for this purpose.

With a nanostructure of an extremely large length-to-diameter ratio and extraordinary strength, CNTs have been considered the ultimate carbon fiber to enhance the mechanical strength of polymer matrices since they were invented in 1991 (Baughman, 2002; Iijima, 1991; Dalton et al., 2003). A multi-walled carbon nanotube was reported to have a tensile strength of 63 GPa (Sinnott and Rodney, 2001; Demczyk et al., 2002). Since carbon nanotubes have a low density for a solid of 1.3–1.4 g/cm^3, their specific strength of up to 48,462 N m/kg is the best of all known materials, much higher compared to that of high-carbon steel 154 kN m/kg. The excellent mechanical properties of carbon nanotubes would make them ideal for composite applications, which would have significant consequences in structural applications and give rise to the assumption that the mechanical properties of the membrane can be improved (Wagner, 2002; Paiva et al., 2004; Duong et al., 2009). CNT-PVA nanocomposite membranes with excellent mechanical properties have been reported by Chen et al. (2005). Their SEM and DSC results showed that the nanotubes were very well wetted by the PVA matrix, which suggested good interfacial bonding between the carbon nanotubes and the PVA polymer matrix. Hu et al. reported a PVA–PVAm membrane incorporated with CNTs for the dehydration of ethylene glycol (Hu et al., 2012). The water permeation flux and separation factor were improved significantly at a low feed water concentration. They also intensively studied the membrane material properties using FTIR, Raman spectroscopy, XRD, contact angle measurement, etc. Peng et al. (2007a,b)) studied the polyvinyl alcohol/carbon nanotube and chitosan-wrapped (CS-wrapped) carbon nanotube hybrid membranes for the pervaporation separation of benzene/cyclohexane mixtures, which exhibited excellent pervaporation properties, as well as a significant improvement in Young's modulus and thermal stability in comparison with PVA membranes without CNTs. They also investigated the free volume characteristics of PVA-CNT nanocomposite membranes by means of a molecular dynamics simulation for the first time. The free volume of PVA-CNT and PVA-CNT(CS) nanocomposite membranes were reported to be distinctly larger than those of the pure PVA membrane and PVA-CS blend membranes, which elucidated that CNTs were functioning as nano-spacers and were an efficient inorganic component to loosen the PVA chain packing and hence to improve the permeation properties of PVA-based membranes.

In order to fully explore the potential of CNTs, they must be well distributed in the membrane casting solutions (Liu et al., 2007). In this work, the effects of CNT pre-treatments, the composition and concentration of the polymer casting solutions, the CNT loading ratio and the ultrasonic mixing protocol were studied with respect to the CNT dispersion and compatibility. The water dispersion of CNTs from five different sources with suitable shapes and sizes for the membrane structure was tested. The procedure for the dispersion of CNTs in the blend solutions was optimized. The CO_2 separation performance of the membrane was tested. Experiments showed that the addition of a small amount of CNTs (1.0 wt.%) in the FSC membrane resulted in an enhanced water swelling capacity and an approximately doubled CO_2 permeance at elevated pressures (10–15 bar), while the CO_2/CH_4 selectivity remained within a similar range as that of the same membrane without CNTs. The reinforcement of the membrane by CNTs is believed to be the reason for the improved membrane performance: the CNTs in the membrane are able to enhance the mechanical strength and stand against part of the compaction effect at elevated pressures, while the nano spacer function of CNTs benefits the swelling process. In addition, the membrane was optimized with respect to the selective layer thickness. The coating layer thickness of the membrane was controlled precisely using the dip-coating method, and membranes with an up-scaled size (300×300 mm) were prepared. The influence of the membrane selective layer thicknesses on separation performance is discussed at various pressures.

2. Experimental

2.1. Materials and membrane casting solution

Polyvinylamine hydrochloride (PVAm HCl) was purchased from Polysciences Inc. (MW 25,000). 90+% hydrolyzed polyvinylalcohol powder (PVA, MW 72,000) was obtained from Merck Schuchardt. Polysulfone (PSf) ultrafiltration flat sheet membranes were provided by Alfa Lava, Denmark. Multi-walled CNTs (diameter 20–80 nm, length 1–2 μm) with a specially tailored size and shape for this work were provided by the catalyst group at the University of Science and Technology (NTNU), which were synthesized on reduced 20 wt.% Fe/Al$_2$O$_3$ prepared by a deposition–precipitation method. The carbon nanotubes were treated with a diluted HF solution or HNO$_3$ solution (both 10% in water) at 298 K with overnight stirring to remove the residue metal and support. The CNTs were oxidized during this acidic treatment. Further details about the preparation and acidic treatment of the multi-walled CNTs can be found in Zhao et al. (2007). In addition, three types of commercially available CNTs from other sources were also investigated: CNTs VGCF-X (15 nm/3 μm) and VGCF-H (150 nm/6 μm) provided by Showa Denko K.K. (SDK, Japan) and MKN-IGCNT-OH5000 (50 nm/10–30 μm) purchased from MKnano (Canada).

To obtain a good dispersion in solutions, CNTs were first sonicated with a pulse ultrasound in a PVAm solution (5 wt.%) at a 40% amplitude for 10 min, then at a 20% amplitude for 60 min. The CNT dispersed PVAm solution was then blended with PVA solution (5 wt.%) at a PVAm/PVA ratio of 4, with a 20% amplitude sonication mixing for 2 min. The samples were cooled during the sonication process. The CNT blended solutions were all filtered with an Acrodisc® syringe filter (pore size 5.0 μm) to remove possible CNT agglomerates.

2.2. Permeation test

The separation performance of the membranes was tested in a gas permeation set-up with a flat sheet type membrane module mounted in a thermostatic cabinet. Details on the permeation experiments can be found in Deng et al. (2009). The relative humidity of the system is adjustable. The relative humidity data were recorded in the retentate stream. Feed gas and sweep gas inlets in the module were designed with a spiral current to enhance the mixing of the gas so as to reduce the possible concentration

polarization on both sides. A relatively high feed gas flow rate was used compared to what was needed for the effective membrane area, and hence the stage-cut of the membrane modules was very small (<0.01); this is to maximize the intrinsic membrane separation performance and minimize the influence of process conditions. Another similar set-up was used to validate the results on a regular basis. The highly repeatable results of both gas permeation set-ups were documented previously in Deng and Hägg (2008). At least one extra sample of each membrane was made and tested in the same conditions to verify the data reported in this paper. Membranes with an effective membrane area of $20\,cm^2$ were tested with synthetic natural gas (10 vol.% of CO_2 in a CO_2/CH_4 gas mixture). The CO_2 permeance (P_{CO_2}) in the units of m^3 (STP)/(m^2 bar h) was calculated using Eq. (2). The selectivity of CO_2 relative to another gas (α) was calculated from the ratio of the permeance of CO_2 and another gas, P_i, by Eq. (3):

$$P_{CO_2} = \frac{q_{p,CO_2}}{A \times \Delta p_{CO_2}} \tag{2}$$

$$\alpha = \frac{P_{CO_2}}{P_i} \tag{3}$$

where ΔP_{CO_2} is the trans-membrane CO_2 partial pressure difference (bar) and q_{p,CO_2} is the permeate flow rate of CO_2, in the unit of m^3 (STP)/h, while A is the effective membrane area, m^2.

2.3. Swelling test

The degree of swelling of the membrane materials was tested in the permeation cell in similar operating conditions as those of the membrane permeation test. Nitrogen with a controlled relative humidity was fed at 2.0 ml/s. The samples were weighed at different relative humidities, including the dry samples, which were weighed after being dried in an N_2 flow overnight; the difference between the masses of the humidified samples and the dry samples caused a gain in the mass of the swollen water. The weights of the samples were recorded after the relative humidity was constant for a minimum of 3 h and had reached water uptake equilibrium. The weight recorded was the average value of three samples in the same conditions. The water swelling degree (SD) of the membrane was calculated according to Eq. (4):

$$SD\,(\%) = \frac{W_s - W_d}{W_d} \times 100 \tag{4}$$

where W_s and W_d are the mass of the swollen and dry membrane materials, respectively.

3. Results and discussion

The defect-free thin nanocomposite CNTs-PVAm/PVA blend selective coating layers on PSf ultrafiltration porous support membranes were prepared following the dip-coating. The membranes were double-coated to eliminate possible pinholes and the penetration of CNTs from the top surface. An SEM image of a dip-coated CNT-PVAm/PVA membrane cross section is given in Fig. 1. The selective layer thickness is 0.7 μm in this membrane. The morphology of the CNTs-PVAm/PVA nanocomposite was observed with a field emission scanning electron microscopy (FESEM, Zeiss Ultra 55 Limited Edition), as shown in Fig. 2. The CNTs were wrapped in the PVAm/PVA polymer, and seemed to be lying parallel to the support substrate surface. This image confirms that the CNTs were wetted by the PVAm/PVA blended solution, and therefore a good dispersion can be expected in the casting solution. In addition, the parallel lying CNTs in Fig. 2 also suggest that a laminated, well-structured CNT framework formed in the coating with 1.0% CNT loading. It has been reported elsewhere that a low concentration of
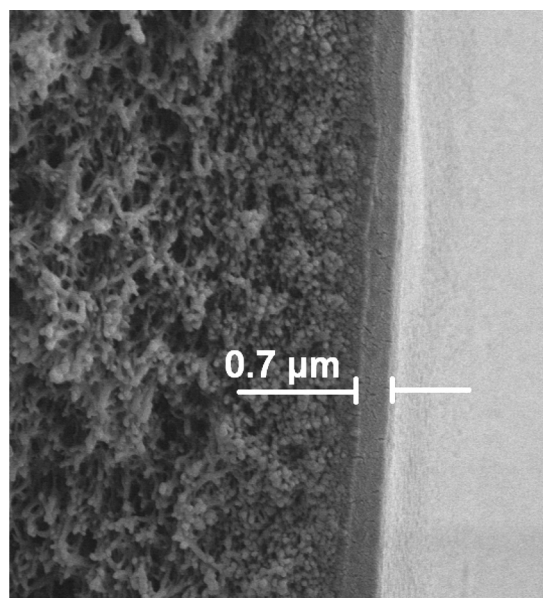

Fig. 1. SEM image of the CNTs-PVAm/PVA membrane, selective layer 0.7 μm.

CNTs in polymer matrices can significantly enhance the mechanical strength of polymer materials (Wagner, 2002; Paiva et al., 2004; Chen et al., 2005; Peng et al., 2007a,b; Guan et al., 2006). For example, 1 wt.% multi-wall CNTs with an enhanced dispersion in a polyethylene film increased the strain energy density by 150% and the ductility by 140% (Ruan et al., 2003), while only 1 wt.% CNT content improved the mechanical response of the methyl–ethyl methacrylate-CNT composites by more than 200%, substantially higher than other reports, where large quantities of CNTs were used (Velasco-Santos et al., 2003). Ideally, the CNT fibers in these reinforced nanocomposite membranes are expected to form laminated structures with an assumed perfectly bonded interface between fiber and matrix, and a loading parallel to the fiber array; thus a transfer of stress from the applied load to the fibers can be achieved, resulting in a fairly uniform stress field in the composite. A simple rule for the ideal mixtures that usually provide a good fit for experiment emerges from the tensile strength of the composite (see Eq.
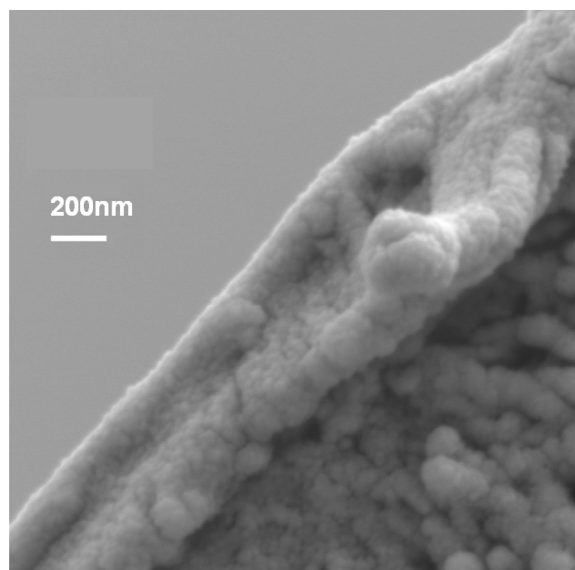

Fig. 2. SEM image of the polymer wrapped CNTs in PVAm/PVA nanocomposite membrane.
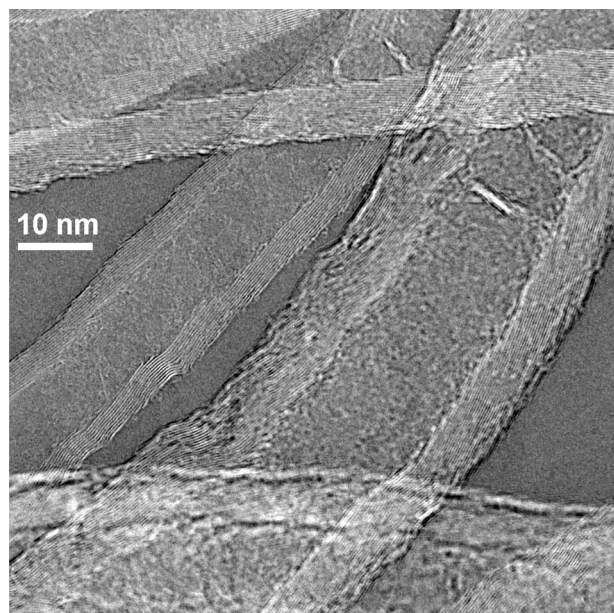
Fig. 3. HRTEM image of HF treated carbon nanotubes, diameter 20–80 nm.

(5), Wagner, 2002), where the subscripts *f* and *m* designate the CNT fiber and the matrix, and *E* and *V* are the tensile strength and volume fraction respectively:

$$E = E_f V_f + E_m V_m \tag{5}$$

The average tensile strength for PVAm/PVA blend samples is 60.53 MPa (Deng et al., 2009). Theoretically, with the addition of 1.0% CNTs (tensile strength approx. 63 GPa), the tensile strength of an ideal nanocomposition membrane could be improved 10-fold – this would be beneficial for the applications of FSC membranes at higher pressures, and could prevent membrane pore filling. Nevertheless, the mechanical strength of the membrane was not determined due to the technical limitations in measuring ultra-thin and highly swollen membranes in this study.

3.1. Dispersion of CNTs in membrane casting solutions

The good dispersion of CNTs in the polymer matrix and a strong adhesion between the CNTs and polymer are the prerequisites for making an effective CNT nanocomposite membrane and taking advantage of the unique mechanical properties of CNTs. As a carbon, CNTs are not hydrophilic by nature, showing very low water affinity. However, the acidic oxidation treatment of the CNT support is found to be a solution to modifying the CNTs for good CNT dispersion in PVAm/PVA blend polymer solutions. Acidic oxidation treatment introduces a large number of functional groups to the surface of the nanotubes, which increases the hydrophilicity of the CNTs (Zhao et al., 2007), making the surface more accessible to the hydrophilic PVAm/PVA blend solutions, and therefore significantly improving the interaction between CNTs and the PVAm/PVA blend polymer. A high-resolution transmission electron microscopy (HRTEM, JEOL 2010F) image of the treated CNTs in Fig. 3

Table 1
Preparation of the CNTs dispersed solution samples.

No.	Samples description			
	Polymer in solution	CNTs in polymer (wt.%)	Acid in CNT treatment	Level of blackness
1[a]	–	1.0	HF	–
2	PVA	1.0	–	1
3	PVAm/PVA	1.0	HF	1
4	PVA	1.0	HNO₃	2
5	PVAm/PVA	1.0	HF	3
6	PVA	2.0	HF	3
7	PVA	1.0	HF	4
8	PVAm (MW 300,000)	1.0	HF	5
9	PVAm (MW 25,000)	1.0	HF	5

[a] Sample 1 is CNTs in distilled water.

shows that no obvious damage takes place during the treatment in an HF solution. A description of the CNT-polymer solution samples is listed in Table 1, and a picture of the listed samples is shown in Fig. 4, in order from a low to a high degree of blackness in solutions of different samples. The degrees of CNT dispersion are rated on 5 levels from no dispersion (level 1) to excellent dispersion (level 5) based on the different levels of the degree of blackness in the CNT solutions. Since the sample solutions were all filtered to remove CNT agglomerates, the degree of blackness should be sufficient to reflect the amount of CNTs dispersed stably in the solutions, and therefore the degree of the CNT dispersion in the solutions.

The experiments performed show that the degree of dispersion of CNTs varies greatly in polymer solutions of different preparation conditions and with different acid treatments of the CNTs. The effect of the two different acidic pre-treatments of CNTs and other aspects that may influence the CNT dispersion were investigated. The solution of CNTs without treatment (No. 2) and treated by HNO₃ (No. 4) or HF (No. 7) in PVA aqueous solutions show that HF treated CNTs have the best dispersion in a PVA solution. The degree of blackness of the samples of HF treated CNTs in distilled water (No. 1), in the PVA solution (No. 6), in the PVAm solution (No. 9), and in the PVAm/PVA blended solution (No. 5) suggested that the dispersion of CNTs in pure PVAm or PVA solutions was better than those in the PVAm/PVA blended solutions, and that the dispersion of CNTs in water was very poor. The interaction of PVAm chains or PVA chains may improve the distribution of CNTs in the solution, and the CNTs may be wrapped in PVAm or PVA chains (as illustrated in Fig. 5). Whereas in the PVAm/PVA blended solution, the strong entanglement of the chains of two polymers may hinder the CNTs from being wrapped in the polymer chains. The PVAm solutions showed better CNT dispersion compared to PVA solutions, which may be due to a better compatibility resulting from the more hydrophilic nature of PVAm chains.

Sample Nos. 6 and 7 are the HF pre-treated CNTs in PVA solution with a CNT content of 1.0% and 2.0%, respectively. A slightly higher degree of blackness in solution No. 7 with 1.0% CNTs was observed, which suggested that the dispersed CNTs in PVA solutions with a higher loading than 1.0% might not cause an increase in the amount of CNTs in PVA solutions. On the contrary, the higher CNT loading in No. 6 might have resulted in agglomerates, and hence more CNTs
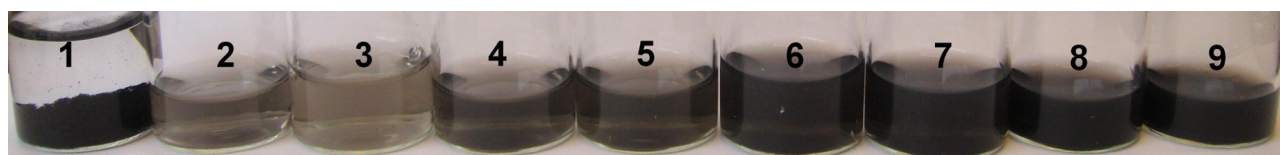

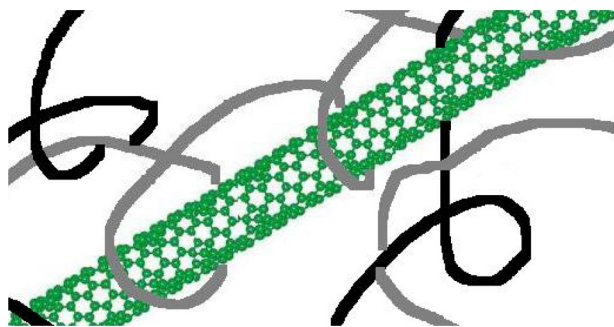**Fig. 4.** CNTs dispersion samples in polymeric solutions.

Fig. 5. Illustration of CNTs wrapped by polymer chains in membrane casting solution.

Fig. 6. Effect of relative humidity on degree of swelling of the PVAm/PVA blend samples with and without CNTs, at atmospheric pressure, room temperature.

were removed from the filters and so showed a lower CNT concentration in the solution. This work then mainly focused on the 1.0% loaded CNT-PVAm/PVA membranes.

All the samples listed in Table 1 were sonicated with pulse ultrasound for 10 min at a 40% amplitude and then sonicated at a 20% amplitude for 60 min (a two-step sonication), except for No. 3, which was only sonicated at a 40% amplitude for 10 min to demonstrate the effect of the sonication procedure. The sonication parameters were optimized in a preliminary study using single-factor tests. Sample Nos. 3 and 5 were CNTs in PVAm/PVA blended solutions using different sonication procedures. It can be seen that the sonication procedure makes a big difference. A sonication procedure with only one step (No. 3) seems to be not sufficient enough to disperse the CNTs. The dispersed CNTs may form agglomerates again if they are not well distributed throughout the polymer solution. The increase of sonication time or amplitude shows no observable improvement to the stability of the dispersion. In the two-step procedure, however, the CNT dispersion seems significantly improved and more stable. The strong sonication in the first step can break the CNT agglomerates, and then the CNT fibers can be better spread among the polymer chains during the gentle sonication for one hour. The two-step sonication procedure was therefore used to thoroughly distribute the CNTs in the casting solution, and to form stable interactions between CNTs and the PVAm/PVA chains.

Nos. 8 and 9 are samples with CNTs in solutions of PVAm with a molecular weight of 340,000 (No. 8) and 25,000 (No. 9). Two samples exhibited a similar degree of blackness or dispersion, and both are the best over all the other samples in the table.

To prepare the CNTs-PVAm/PVA membrane for up-scaling and potential industrial applications, the specially tailored CNTs were replaced with commercially available CNTs at a later stage. Three types of commercially available CNTs from other sources were investigated, which were selected from a screen process for water dispersible CNTs. CNTs VGCF-X (15 nm/3 μm) and VGCF-H (150 nm/6 μm) were provided by Showa Denko K. K. (Japan), and MKN-IGCNT-OH5000 (50 nm/10–30 μm) was purchased from MKnano (Canada). The VGCF series showed a comparable CNT dispersion in the PVAm/PVA solutions to the tailor-made CNTs from NTNU when following the same procedure in dispersion. The solutions showed the same degree of blackness as the solution described as the 5th level of blackness in Table 1, and were stable over a 1 month observation. Although longer than the VGCF CNTs and NTNU CNTs, the MKnano CNTs (10–30 μm) were also found to be well distributed in the blend polymer solution and to be stable. The kind of CNT and the hydrophilicity of the CNT surface seem to have played a more important role than the length of the fibers within the range of this study. However, due to the limitations of the very thin membrane coating for the current work, only
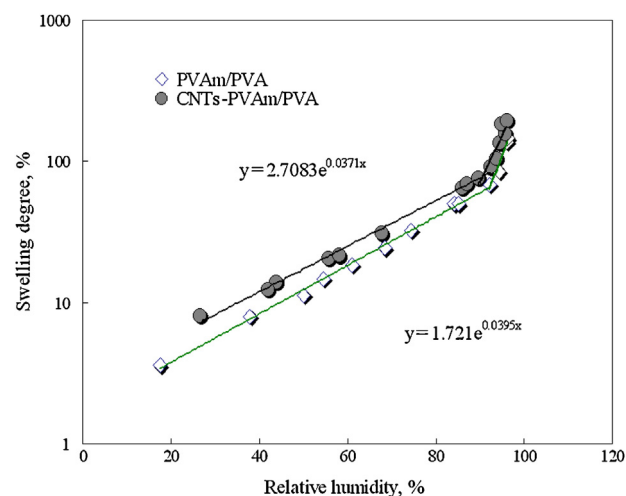
the VGCF-X (15 nm/3 μm) CNTs were used to prepare membranes for further study in order to ensure a defect-free coating layer.

3.2. Effect of CNT addition on water swelling capacity

A comparison of the water swelling capacity of the PVAm/PVA blend polymer samples with and without the addition of the CNTs is illustrated in Fig. 6. It can be seen that the degree of swelling of both samples increased with the relative humidity in a similar trend, following exponential relationships in two stages. Details about the two-stage swelling behavior of hydrogels can be found in Kim et al. (1992), Chen et al. (1998) and Deng and Hägg (2010a). The equations for the curve fittings for the degree of swelling which took place at the first stage are expressed in Fig. 6 with a relative humidity within a range of 20–92%. Both the experimental data and the simulated equations show that the degree of water swelling of the CNTs-PVAm/PVA blend nanocomposite samples was higher than that of its counterpart sample at the same relative humidity. This is believed to be the nano-spacer function of the CNTs, which introduces extra space into the polymer framework to hold more water in the polymer. A deviation of the experimental swelling data from the exponential equations occurred (relative humidity > 92%), where the growth of the degree of swelling of both samples started to increase much more quickly with the increasing relative humidity. These exponential relationships of the degree of swelling with relative humidity suggest that an increase in relative humidity favors the swelling of the membrane more in a higher relative humidity range, and the degree of swelling of the CNTs-PVAm/PVA sample remains higher than that of its counterpart.

Fig. 7 presents the normalized degree of swelling of a CNT reinforced membrane to that of its counterpart at different operating pressures. The degrees of swelling of both samples were calculated based on the relative humidity–swelling degree relationship indicated in Fig. 6 and the highest relative humidity data recorded in the separation processes of the membranes at different pressures. Since the polymer framework becomes compacted at increased pressures, the constants in the relative humidity–swelling degree relationship obtained based on atmospheric pressure can change. The data shown in Fig. 7 is therefore the normalized degree of swelling of the CNTs-PVAm/PVA composite sample compared to that of the PVAm/PVA blend sample at the same pressure, in order to diminish possible errors in the comparison of the swelling of the two samples at elevated pressures. Both membranes experienced a decreased degree of swelling with increasing operating pressure
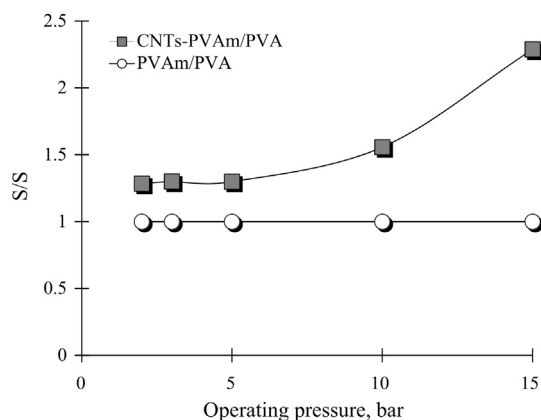
Fig. 7. Effect of operating pressures on degree of swelling of the PVAm/PVA blend samples with and without CNTs.

due to the compaction effect. However, as can be seen in Fig. 7, the degree of swelling of the CNT reinforced nanocomposite membrane exhibited higher swelling capacities, especially at elevated pressures, where a 1–2 fold greater swelling was found at 10 bar and 15 bar in this test. It is therefore reasonable to assume that the compaction effect on the CNT reinforced membrane under pressurization is less than that of its counterpart membrane without CNTs.

3.3. The CO_2/CH_4 separation performance

The CO_2/CH_4 separation at 2 bar and room temperature (25 °C) was performed with a CNTs-PVAm/PVA blend nanocomposite membrane. A synthetic natural gas CO_2/CH_4 mixture was used. The selective layer thickness of 0.7 μm in this membrane was confirmed with SEM images (see Fig. 1). The separation performance of this membrane is presented in Fig. 8. As can be seen in Fig. 8(a), a CO_2/CH_4 selectivity of 45 was achieved at a relative humidity of 88% in the CNTs-PVAm/PVA membrane, and then the selectivity shows a slight decrease and reaches 42 at a relative humidity of 92%. Fig. 8(b) shows an exponential increase of CO_2 permeance depending on the relative humidity in the membranes. It reached a maximum of 0.35 m³ (STP)/(m² h bar) at the maximum relative humidity (92%) in the CNTs-PVAm/PVA membrane, where the CO_2/CH_4 selectivity was 42. The separation performance of the counterpart PVAm/PVA blend membrane is also plotted in Fig. 8 for comparison. The CO_2 permeance of the CNTs-PVAm/PVA blend nanocomposite membrane was found to improve by approximately 30%, which is consistent with the enhanced degree of swelling in the CNT reinforced PVAm/PVA blend shown in Fig. 6. The selectivity of both membranes decreasing within the high relative humidity range may be due to the loose structure of the membranes in a highly swollen state, as well as the increased CH_4 permeance caused by the loss of the sieving effect on the swollen membranes. However, the CNTs-PVAm/PVA membrane showed an apparently improved CO_2/CH_4 selectivity within the high relative humidity range compared to its counterpart. The selectivity improved from 32 to 42 at a relative humidity of 92%, which is a big advantage to the separation process, since the highest CO_2 permeance is usually reached at the highest relative humidity, and the optimal relative humidity for separation is generally the highest possible relative humidity that the separation system can obtain.

The influences of operating pressure and relative humidity on the CO_2 permeance of the CNTs-PVAm/PVA membrane and its counterpart membrane without the addition of CNTs are illustrated in Fig. 9. The CO_2 permeances are plotted as a function of relative humidity at different operating pressures, i.e. 3, 5, 10 and 15 bar.
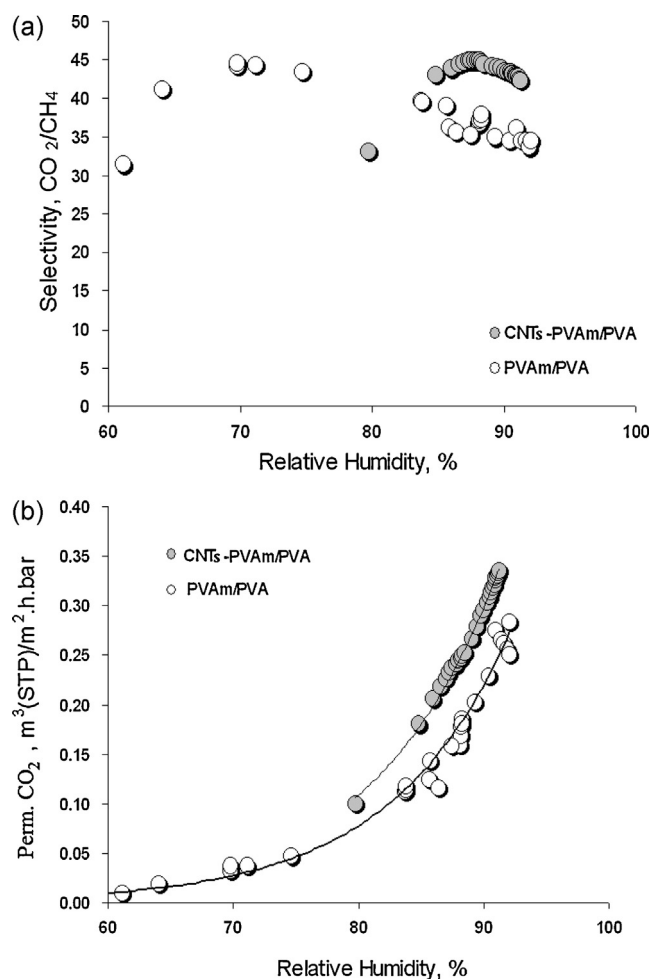

Fig. 8. Effect of relative humidity on CO_2/CH_4 selectivity (a) and CO_2 permeance (b) of the CNTs-PVAm/PVA membrane and PVAm/PVA membrane, at 2 bar and 25 °C.

From Fig. 9 it can be seen that at the same operating pressure, the CNT reinforced PVAm/PVA membrane exhibited a notably higher CO_2 permeance compared with that of the membrane without CNTs, especially at 10 and 15 bar, where the CO_2 permeances are more than doubled in the CNT reinforced membrane. The CO_2 permeance of the CNT-PVAm/PVA membrane is also higher at the same
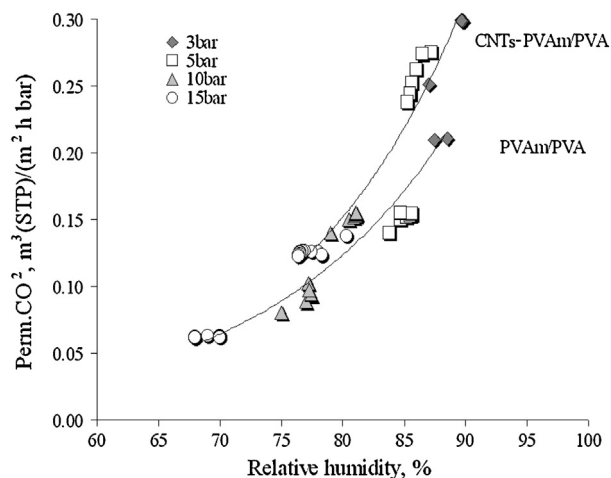

Fig. 9. Effect of relative humidity and operating pressure on CO_2 permeance of the CNTs-PVAm/PVA membrane and PVAm/PVA membrane, at 3–15 bar, 25 °C.
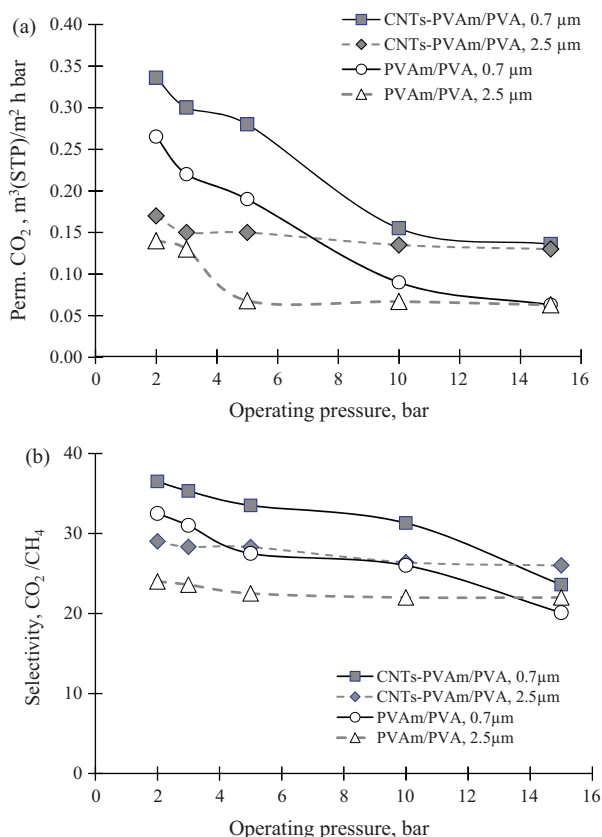
Fig. 10. Effect of operating pressure on CO_2 permeance (a) and CO_2/CH_4 selectivity (b) of the CNTs-PVAm/PVA membrane and PVAm/PVA membrane, at 2–15 bar, 25 °C.

relative humidity. The significantly improved CO_2 permeance of the CNT reinforced membrane suggests that the addition of CNTs into a membrane may have not only resulted in a better swelling capacity, but also in a better mechanical strength against the compaction effect at high pressures.

3.4. Effect of membrane selective layer thickness

In general, a decrease in the membrane selective layer thickness can reduce the overall gas transport resistance, and therefore increase the gas permeance. The situation is similar in the PVAm/PVA membranes at low pressures (2–5 bar in this study), and a thinner PVAm/PVA membrane usually exhibits a higher gas permeance with higher, or at least maintained, CO_2 selectivity over other gases. However, experiments show that operating pressures exhibit different effects on CO_2 permeation through membranes with different thicknesses in these membranes, and the CO_2 permeance has a tendency to decrease with increasing pressure. Fig. 10 presents the effects of operating pressures on the CO_2 separation performance of the CNT reinforced PVAm/PVA membrane and its counterpart membrane in two different selective layer thicknesses. In Fig. 10(a), the CO_2 permeance of the CNT-PVAm/PVA membrane and the PVAm/PVA membranes with selective layer thicknesses of 0.7 μm and 2.5 μm are plotted as a function of operating pressure. Please note that in Fig. 10, only the highest CO_2 permeances for each membrane is plotted at various pressures, where the relative humidities for the datum points are different. Some points can be found in Fig. 9: The data for the membranes of 0.7 μm are shown in Fig. 9 to relate the separation performance to the relative humidity. As can be seen in Fig. 10(a), the CO_2 permeances of the membranes all decrease with increasing operating pressures, showing the characteristic of the CO_2 facilitated transport mechanism (Deng et al.,

2009; Matsuyama et al., 1999). The plots of the CNT reinforced PVAm/PVA membranes are higher than those of their counterparts of the same thickness, suggesting that the addition of CNTs to the PVAm/PVA improved the separation performance, especially at higher pressures. For example, the CNT reinforced membranes had a nearly 2-fold increased CO_2 permeance at 15 bar compared to their counterparts. This figure also shows that the effect of pressure on CO_2 permeance varies in membranes of different selective layer thickness. The membranes with thinner selective layers exhibit significantly higher CO_2 permeances at low pressures and decrease more quickly with increasing pressures, while the CO_2 permeance of thicker membranes are more stable. The CO_2 permeance differences are big in both types of membrane at low pressures (2–5 bar), whereas when the feed pressure increases to 10 and 15 bar, membranes with selective layer thicknesses of 0.7 μm and 2.5 μm exhibit comparable CO_2 permeance. These trends suggest that thinner membranes are more vulnerable to the effects of pressure. Concentration polarization may have also partly contributed to the faster decrease of CO_2 permeance with increasing feed pressure in the thinner membranes than the thicker ones. Due to the very high CO_2 permeance in this facilitated transport membrane, the concentration polarization effect is not negligible, which results in a reduced driving force and hence decreased gas permeance. One way to minimize this, is to use high flow rate sweep gas. The tangential direction feed/sweep inlet and very low stage-cut can also reduce the negative effect. However, the concentration polarization could not be thoroughly eliminated, especially in the thin membranes with very high CO_2 permeance.

Fig. 10(b) shows the selectivities of the membranes. At low pressures, thinner membranes exhibit higher selectivities. However, thicker membranes have a more stable selectivity toward pressure change. When the pressure increases to 15 bar in this test, the selectivities of the thicker membranes become higher than those of their thinner counterparts. The optimal thickness of the membrane selective layer seems different for separations at different operating pressures. For operating at elevated pressures (i.e. 15 bar) in this test, a CNT reinforced membrane with a thickness of 2.5 μm is preferred. These membranes follow the same trend as the PVAm/PVA membrane previously reported in Deng et al. (2009) for CO_2/N_2 separation. This phenomenon can be explained by the facilitated transport mechanism; the competition between the Fickean diffusion and the complexation reaction in the facilitated transport is the main reason. To maintain a sufficiently facilitated transport effect, thicker membranes (and hence more facilitated transport carriers) are needed. Theoretically, an optimized thickness can be estimated using the 'second Damköhler number' (Mulder, 2003). The compaction of membranes at increased pressures also contributes to the effect of pressure on separation performance. It is reasonable to assume that thicker membrane coating layers may be required for higher pressures ($P > 15$ bar).

The solution casting method is commonly used to prepare lab scale membranes. However, membrane coating layers were found to be uneven, and the thicknesses very difficult to control in preparing a CNTs-PVAm/PVA membrane, especially when membranes of an up-scaled size were considered. A dip-coating procedure was therefore developed and used throughout this study. The wettability of the solution on the support is a crucial prerequisite in using this method, but it is not a concern for this membrane, since the hydrophobic groups ($-OCCH_3$) of the partially hydrolyzed PVA (90+% hydrolyzed) in the PVAm/PVA blend aqueous solution can reduce the surface tension and provides good contact between the cast solution and the support surface, which enables the formation of the ultra-thin coating on the PSf support. The membranes were double-coated to eliminate any possible defects or the branching out of the CNTs from the coating surface. According to the Navier–Stokes equation (Mulder, 2003), the coating layer
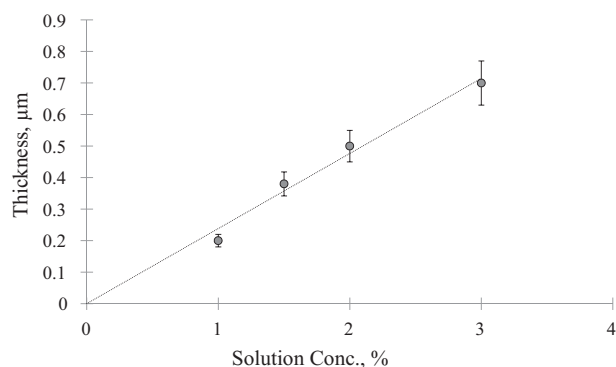
Fig. 11. Effect of casting solution concentration on coating layer thickness of the dip-coated membranes.

thickness is generally proportional to the volume fraction of polymer in the solution in dip-coating. The effects of the concentration of casting solutions and the coating layers on thickness in the CNTs-PVAm/PVA membrane were investigated. An almost linear relationship was found between the casting solution concentration and membrane thickness, as shown in Fig. 11. Membranes of an up-scaled size (300×300 mm) were prepared with even coatings using the developed dip-coating procedure in this study.

4. Conclusion

The CNT reinforced PVAm/PVA membrane combines the advantages of the excellent CO_2-selective separation performance of FSC membranes and the good mechanical properties of CNTs, as well as its nano spacer function in the composite membrane. The CNTs may have formed a laminated structure in the PVAm/PVA blend polymer framework. The uniformly dispersed CNTs in the PVAm/PVA blends reduced the compaction effect of the membrane at elevated pressures, and the nano spacer function of the CNTs brought in an enhanced swelling capacity of the CNTs-PVAm/PVA blend nanocomposite, which significantly improved the CO_2 separation performance of the membrane. A selectivity of CO_2/CH_4 of up to 45, and a CO_2 permeance of up to 0.35 m^3 (STP)/m^2 h bar was documented within the low pressure range. Membranes with varied coating layer thicknesses influenced the membrane separation performance differently at different operating pressures. Thicker membranes are generally favorable for higher pressures – this was documented up to 15 bar.

The operating humidity and degree of swelling of this facilitated transport membrane significantly influenced the membrane separation performance. For pressures higher than the tested range in this paper, the swelling capacity of the membrane material may well be further improved, and a higher loading of CNTs in the membrane materials could be one approach. Further work can be done to improve the dispersion of CNTs in the casting solution to achieve a higher CNT loading; for instance, by introducing CNTs with a higher compatibility with the PVA and PVAm blend solution.

Acknowledgements

References

Adewole, J.K., Ahmad, A.L., Ismail, S., Leo, C.P., 2013. Current challenges in membrane separation of CO_2 from natural gas: a review. Int. J. Greenhouse Gas Control 17, 46–65.

Baughman, R.H., 2002. Carbon nanotubes – the route toward applications. Science 297, 787–792.

Chen, W.-L., Shull, K.R., Papatheodorou, T., Styrkas, D.A., Keddie, J.L., 1998. Equilibrium swelling of hydrophilic polyacrylates in humid environments. Macromolecules 32, 136–144.

Chen, W., Tao, X., Xue, P., Cheng, X., 2005. Enhanced mechanical properties and morphological characterizations of poly(vinyl alcohol)-carbon nanotube composite films. Appl. Surf. Sci. 252, 1404–1409.

Cussler, E.L., 1997. Diffusion Mass Transfer in Fluid Systems. Cambridge University Press, Cambridge.

Dalton, A.B., Collins, S., Munoz, E., Razal, J.M., Ebron, V.H., Ferraris, J.P., Coleman, J.N., Kim, B.G., Baughman, R.H., 2003. Super-tough carbon-nanotube fibres. Nature 423, 703.

Demczyk, B.G., Wang, Y.M., Cumings, J., Hetman, M., Han, W., Zettl, A., Ritchie, R.O., 2002. Direct mechanical measurement of the tensile strength and elastic modulus of multiwalled carbon nanotubes. Mater. Sci. Eng. A 334, 173–178.

Deng, L., Hägg, M.-B., 2008. PVA/PVAm blend FSC membrane for natural gas sweetening. In: 1st Annual Gas Process Symposium Proceeding.

Deng, L., Hägg, M.-B., 2010a. Swelling behavior and gas permeation performance of PVAm/PVA blend FSC membrane. J. Membr. Sci. 363 (1–2), 295–301.

Deng, L., Hägg, M.-B., 2010b. Techno-economic evaluation of biogas upgrading process using CO_2 facilitated transport membrane. Int. J. Greenhouse Gas Control 4, 638–646.

Deng, L., Kim, T.-J., Hagg, M.-B., 2006. PVA/PVAm blend FSC membrane for CO_2-capture. Desalination 199, 523–524.

Deng, L., Kim, T.-J., Hägg, M.-B., 2009. Facilitated transport of CO_2 in novel PVAm/PVA blend membrane. J. Membr. Sci. 340, 154–163.

Duong, H.M., Yamamoto, N., Papavassiliou, D.V., Maruyama, S., Wardle, B.L., 2009. Inter-carbon nanotube contact in thermal transport of controlled-morphology polymer nanocomposites. Nanotechnology 20, 155702.

Guan, H.-M., Chung, T.-S., Huang, Z., Chng, M.L., Kulprathipanja, S., 2006. Poly(vinyl alcohol) multilayer mixed matrix membranes for the dehydration of ethanol–water mixture. J. Membr. Sci. 268, 113–122.

Hu, S.Y., Zhang, Y., Lawless, D., Feng, X., 2012. Composite membranes comprising of polyvinylamine–poly(vinyl alcohol) incorporated with carbon nanotubes for dehydration of ethylene glycol by pervaporation. J. Membr. Sci. 417–418, 34–44.

Iijima, S., 1991. Helical microtubules of graphitic carbon. Nature 354, 56–58.

Kim, J.H., Kim, J.Y., Lee, Y.M., Kim, K.Y., 1992. Properties and swelling characteristics of cross-linked poly(vinyl alcohol) chitosan blend membrane. J. Appl. Polym. Sci. 45, 1711–1717.

Kim, T.-J., Vrålstad, H., Sandru, M., Hägg, M.-B., 2013. Separation performance of PVAm composite membrane for CO_2 capture at various pH levels. J. Membr. Sci. 428, 218–224.

Liu, J.Q., Xiao, T., Liao, K., Wu, P., 2007. Interfacial design of carbon nanotube polymer composites: a hybrid system of noncovalent and covalent functionalizations. Nanotechnology 18, 165701.

Liu, L., Chakma, A., Feng, X., 2008. Gas permeation through water-swollen hydrogel membranes. J. Membr. Sci. 310, 66–75.

Matsuyama, H., Terada, A., Nakagawara, T., Kitamura, Y., Teramoto, M., 1999. Facilitated transport of CO_2 through polyethylenimine/poly(vinyl alcohol) blend membrane. J. Membr. Sci. 163, 221–227.

Mulder, M., 2003. Basic Principles of Membrane Technology. Kluwer Academic Publishers Inc., Netherlands.

Paiva, M.C., Zhou, B., Fernando, K.A.S., Lin, Y., Kennedy, J.M., Sun, Y.P., 2004. Mechanical and morphological characterization of polymer-carbon nanocomposites from functionalized carbon nanotubes. Carbon 42, 2849–2854.

Peng, F., Hu, C., Jiang, Z., 2007a. Novel ploy(vinyl alcohol)/carbon nanotube hybrid membranes for pervaporation separation of benzene/cyclohexane mixtures. J. Membr. Sci. 297, 236–242.

Peng, F., Pan, F., Sun, H., Lu, L., Jiang, Z., 2007b. Novel nanocomposite pervaporation membranes composed of poly(vinyl alcohol) and chitosan-wrapped carbon nanotube. J. Membr. Sci. 300, 13–19.

Ruan, S.L., Gao, P., Yang, X.G., Yu, T.X., 2003. Toughening high performance ultrahigh molecular weight polyethylene using multiwalled carbon nanotubes. Polymer 44, 5643–5654.

Sandru, M., Haukebø, S.H., Hägg, M.-B., 2010. Composite hollow fiber membranes for CO_2 capture. J. Membr. Sci. 346, 172–186.

Sinnott, S.B., Rodney, A., 2001. Carbon nanotubes: synthesis, properties, and applications. J. Crit. Rev. Solid State Mater. Sci. 26, 145–249.

Velasco-Santos, C., Martinez-Hernandez, A.L., Fisher, F., Ruoff, R., Castano, V.M., 2003. Dynamical–mechanical and thermal analysis of carbon nanotube-methyl–ethyl methacrylate nanocomposites. J. Phys. D: Appl. Phys. 36, 1423–1428.

Wagner, H.D., 2002. Reinforcement. Encyclopedia of Polymer Science and Technology, vol. 4., 3rd ed. John Wiley & Sons, Inc, New York, pp. 94–115.

Zhang, Y., Sunarso, J., Liu, S., Wang, R., 2013. Current status and development of membranes for CO_2/CH_4 separation: a review. Int. J. Greenhouse Gas Control 12, 84–107.

Zhao, T.-J., Sun, W.-Z., Gu, X.-Y., Rønning, M., Chen, D., Dai, Y.-C., Yuan, W.-K., Holmen, A., 2007. Rational design of the carbon nanofiber catalysts for oxidative dehydrogenation of ethylbenzene. Appl. Catal. A: Gen. 323, 135–146.